Materials Engineering and Technologies

https://met.cultechpub.com/met

Cultech Publishing

Article

Thermal Stability and Corrosion Protection of Graphene Nanocoating's on Steel: Experimental Analysis and A Molecular Dynamics Study

Surajudeen Sikiru[1,2*], Syafiq Bin Safarudin[1]

[1]School of Physics and Materials Studies, Faculty of Applied Sciences, Universiti Teknologi Mara, Shah Alam, Selangor, Malaysia

[2]Sustainable Energy Materials Laboratory, Faculty of Applied Sciences, Universiti Teknologi MARA, Shah Alam, Selangor Darul Ehsan, Malaysia

Corresponding authors: Surajudeen Sikiru, surajudeen86@gmail.com/ surajudeen@uitm.edu.my

Abstract

Graphene-based nanocoating's are gaining attention as protective barriers for steel, particularly in offshore pipeline systems exposed to harsh conditions. Traditional coatings struggle with thermal stability and adhesion at high temperatures, limiting their corrosion resistance. This research investigates the thermal stability, structural integrity, and protective effectiveness of graphene nanocoating's applied to steel substrates using a dip-coating technique. Simulations conducted with Materials Studio across temperatures from 393 to 633 K revealed strong adhesion between graphene and steel, demonstrated through high adsorption energy values. At lower temperatures (393 K), the Van der Waals energy was measured at –30.77 kcal/mol, indicating strong attractive interactions. As temperature increased, these values varied but remained negative, confirming ongoing non-covalent interactions. The intramolecular energy consistently measured at 478.81 kcal/mol, highlighting the graphene layer's structural stability under heat stress. Experimental validation included X-ray diffraction (XRD) which confirmed graphite's oxidation to graphene oxide, Fourier transform infrared spectroscopy (FTIR) which identified functional groups from p-phenylenediamine, and scanning electron microscopy (SEM) revealing a wrinkled layered morphology for effective surface coverage. Further electrochemical impedance spectroscopy and salt immersion studies indicated enhanced corrosion resistance. Overall, graphene nanocoating's exhibit exceptional thermal stability, mechanical strength, and chemical resistance, making them promise for long-term protection of offshore pipeline steel.

Keywords

Corrosion, Materials Studio software, Offshore pipeline, Graphene, Adsorption energies, Nanocoating's

Article History

Received: 22 July 2025 **Revised:** 30 October 2025
Accepted: 05 November 2025 **Available Online:** 11 November 2025

1. Introduction

Offshore oil and gas exploration has become an increasingly vital component of the global energy landscape, supplying a significant portion of the world's fossil fuel demand [1, 2]. These operations, often situated in harsh marine environments, are heavily dependent on an intricate network of pipelines to transport extracted hydrocarbons from seabed's to processing facilities [3]. Despite their critical role, offshore pipelines are continuously exposed to extreme conditions saltwater immersion, fluctuating temperatures, high pressure, and microbial activity all of which pose severe threats to their structural integrity [4]. Among the most pressing challenges in this context is corrosion, a natural but costly degradation process that compromises pipeline performance, safety, and lifespan. Corrosion in offshore environments is not merely a maintenance issue; it represents a significant economic burden and a potential environmental hazard [4]. Pipeline failures due to corrosion can lead to catastrophic oil spills, jeopardizing marine ecosystems and incurring massive cleanup costs. The industry has traditionally relied on protective coatings, cathodic protection systems, and periodic maintenance to mitigate corrosion [5, 6]. However, the effectiveness of these conventional methods is often limited by the aggressive and unpredictable nature of marine conditions. Consequently, there is a growing imperative to develop next-generation protective solutions that can offer robust, long-term resistance to corrosion while remaining cost-effective and environmentally sustainable [7, 8]. In recent years, nanotechnology has emerged as a promising frontier in materials science, offering novel solutions to age-old engineering problems. One of the most intriguing developments in this field is the advent of graphene-based nanocoating's [9]. Graphene, a single layer of carbon atoms arranged in a hexagonal lattice, boasts a remarkable set of properties: exceptional mechanical strength, superior thermal and electrical conductivity, and, most pertinently, high chemical inertness [10]. These attributes make graphene an ideal candidate for enhancing the protective capabilities of anti-corrosion coatings. Therefore, the continued development of improved anti-corrosion coatings is vital to prolonging the life and performance of such offshore pipelines. An example of how an offshore pipeline system is being utilized in an industrial workplace can be seen in Figure 1. Previous studies on offshore pipeline corrosion largely focus on conventional coatings or preliminary graphene-based applications without fully addressing their long-term behavior under harsh marine conditions. While experimental investigations have demonstrated graphene's anti-corrosion potential, challenges such as scalability, uniform dispersion, and durability remain unresolved. Moreover, most prior works emphasize laboratory tests, which are time-consuming and limited in scope. The current study differs by employing advanced simulation techniques finite element analysis and molecular dynamics to predict graphene-based coating performance, optimize configurations, and identify potential failure mechanisms. This simulation-driven approach bridges the gap between theoretical material potential and real-world offshore pipeline applications.

Figure 1. An offshore pipeline system Copyright Clearance Center, Provided by American Chemical Society License Number (6106280148750) [11].

Unlike traditional coatings, which can become porous or delaminate over time, graphene-based coatings form ultra-thin, impermeable barriers that can significantly slow down or even prevent the diffusion of corrosive agents such as water, oxygen, and chloride ions [12-14]. Furthermore, the high surface area of graphene allows for strong adhesion to metal substrates and compatibility with other nanomaterials or polymers, enabling the creation of composite coatings tailored to specific operational needs [15-17]. These advantages have sparked a surge of interest in exploring graphene's potential as a transformative material in corrosion-resistant technologies. However, the practical deployment of graphene-based coatings in offshore environments is not without its challenges [18, 19]. Issues such as uniform dispersion of graphene in matrix materials, scalability of production, and long-term durability under real-world marine conditions remain areas of active investigation [20, 21]. Moreover, experimental approaches to studying corrosion protection are often time-consuming, resource-intensive, and constrained by laboratory limitations. This is where simulation analysis becomes a powerful tool. Simulation techniques, particularly those grounded in computational modeling, allow researchers to predict and visualize the behavior of graphene-based nanocoating's under varying

environmental stressors [12]. Through finite element analysis (FEA), molecular dynamics (MD), and other multi-scale modeling approaches, it is possible to assess key performance indicators such as adhesion strength, barrier effectiveness, and degradation rates over extended periods. Simulation also facilitates the optimization of coating formulations, thicknesses, and application methods before moving into costly physical testing stages. This study leverages simulation analysis to explore the development and performance of graphene-based nanocoating's designed specifically for offshore pipeline applications. By modeling the interactions between the coating layers and the corrosive agents present in marine environments, this research aims to uncover the mechanisms by which graphene enhances corrosion resistance. It also seeks to identify potential failure modes and design improvements that could be implemented in real-world conditions. The objectives of this research are threefold: (1) to simulate the structural and chemical behavior of graphene-based coatings under offshore environmental stress, (2) to evaluate their effectiveness in reducing corrosion rates compared to conventional coatings, and (3) to propose optimized coating configurations for future experimental validation and industrial application. Through this integrated approach, the study aspires to contribute valuable insights into the role of advanced nanomaterials in safeguarding critical offshore infrastructure. In a broader context, the successful development of high-performance graphene-based nanocoating's aligns with global efforts to enhance the sustainability and resilience of energy infrastructure. As the demand for offshore resources continues to grow and environmental regulations tighten, industries must adopt innovative materials and technologies that ensure both operational efficiency and environmental stewardship. Graphene, with its multifunctional capabilities, stands at the intersection of these imperatives, offering a compelling path forward in the battle against corrosion. In summary, this research presents a forward-looking investigation into the potential of graphene-based nanocoating's to revolutionize corrosion protection in offshore pipeline systems. Through simulation-driven analysis, it seeks to bridge the gap between theoretical potential and practical application, paving the way for more durable, safe, and sustainable energy infrastructure in the face of increasingly complex environmental challenges.

2. Computational Approach

To investigate the corrosion resistance properties of graphene-based nanocoating's on steel substrates, simulations were performed using Materials Studio software. The simulation aimed to assess key energy parameters adsorption energy, Van der Waals energy, and intramolecular energy across a range of temperatures, providing insights into the coating's performance under varying offshore conditions [22, 23]. The process began by constructing a graphene monolayer model using the Visualizer module. A slab model of a representative steel surface was generated to serve as the substrate. The graphene layer was then positioned parallel to the steel surface, maintaining an appropriate distance to allow interaction without initial overlap. Geometry optimization was performed using the Forcite module, employing the COMPASS force field to accurately represent interatomic interactions [24]. To simulate the temperature influence, molecular dynamics (MD) simulations were conducted at seven temperature points: 393 K, 433 K, 473 K, 513 K, 533 K, 593 K, and 633 K. Each system was equilibrated under the volume constant temperature (NVT) ensemble using a Nose-Hoover thermostat, ensuring constant volume and temperature throughout the simulation [25, 26]. A simulation time of 100ps was adopted for each temperature, with a time step of 1 fs to maintain system stability and capture atomic-level behavior. The adsorption energy was calculated using the total energy differences between the combined system (graphene + steel), the isolated graphene sheet, and the clean steel surface [27, 28]. Van der Waals energies were extracted from the non-bonded interaction data, reflecting the strength of physical interactions. Intramolecular energy values, representing the internal bonding stability of the graphene sheet, were monitored across all simulations. This computational approach provides a comprehensive understanding of how graphene interacts with steel at various temperatures. The stability of the graphene-steel interaction, even under elevated thermal conditions, supports its potential as a corrosion-resistant coating for offshore pipelines. The use of Materials Studio allowed for precise control over simulation parameters and detailed analysis of energy behavior, forming a robust framework for further nanocoating optimization studies.

2.1 Materials and Graphene Oxide Synthesis

In this research study, graphite powder, sodium nitrate ($NaNO_3$), potassium permanganate ($KMnO_4$), sulphuric acid (H_2SO_4), hydrogen peroxide (H_2O_2), ethanol (C_2H_5OH), ultra-pure water, hydrochloric acid (HCl), aniline, ammonium persulfate (APS), p-phenylenediamine, epoxy resin (Morcote BJC 39 - Part A) + (BJC Hardener - Set B) as coating matrix, sodium chloride (NaCl), methanol (CH_3OH) were used. To obtain graphene as a material, it must first be synthesized. For some time now, graphene has been a rising topic among material scientists; thus, several methods have been discovered for the exfoliation of graphite into graphene for the synthesis process. The method of synthesizing graphene in this project involves the chemical exfoliation process, also known as Hummers' Method, a top-down approach for synthesizing nanomaterials.

By using the Modified Hummers' Method [29], graphene oxide can be synthesized from graphite powder. 69ml of H_2SO_4 was added to a mixture of 3.0g of graphite powder and 1.5g of $NaNO_3$. The mixture was then stirred and cooled in an ice bath to maintain its temperature below 288.15K. Then, 9.0g of $KMnO_4$ was added in portions to the mixture to maintain its temperature from excess heat due to the exothermic reaction and left to stir for 6 hours. An additional 9.0 g of $KMnO_4$ was added in one whole portion and stirred for 12 hours a temperature 308.15K of 200 ml of deionized water was added and cooled to room temperature. 30ml of H_2O_2 was added to halt the oxidation process completely.

100ml of 5% HCl was added to remove any excess metal ions and other impurities that may affect the oxidation degree of graphene oxide. Ethanol and deionized water were added simultaneously to the solution mixture during centrifugation (3 cycles, each 6000 rpm for 20 minutes) until a sedimentation of suspended graphene oxide particles was obtained. The suspended GO is placed in a petri dish to be dried in a vacuum oven for 12-18 hours at a temperature of 333.15K, resulting in a yield product of 3.0g of GO.

2.2 Substrates for Nano-Coating Application

Carbon steel substrates (2 x 2 x 0.5 cm) were used as the simulation to model the surface of offshore pipelines in this research study. To prepare the substrates, first, they were polished with abraded sandpapers with grades of 180, 320, and 1000 on a wet grinding machine. The substrates were then immersed in ethanol and methanol baths to remove dust or impurities on the surface while aided by ultrasonication. A total of 8 carbon steel substrates were used in this study. 0.5 g of p-Phenylenediamine (PPD) substance was diluted in 25 ml of ultra-pure water and was stirred and heated to 303.15K to complete dissolution. The mass ratio used for (GO/PPD) was 1:1. 0.5 g of GO was also placed in 25 ml of ultra-pure water and immersed in an ultrasonic bath for 1 hour to disperse GO particles efficiently. Then, both solutions were mixed and stirred at 353.15K for 30 minutes to complete the reduction and functionalization of GO. It was then washed through centrifuging in ultra-pure water until its color changed from purple to colorless. The suspension of PPD-GO particles was collected and dried in a vacuum oven at 313.15K for 12 hours. A yield product of 0.25g of PPD-GO was obtained. Separately, under ice bath conditions, 1 g of GO was added to 25 ml of ultra-pure water and sonicated for 30 minutes to obtain a better-dispersed solution of GO particles. Then, 2.33 g of aniline monomer was added to the GO solution. 2 g of ammonium persulfate (APS) was dissolved in 40 ml of 1M HCl and stirred for 10-20 minutes. The APS solution was added to the PANI/GO solution dropwise and stirred in an ice bath for 6 hours. The solution was then washed repeatedly in ethanol and ultra-pure water by centrifuging until it turned colorless. The suspension of PANI-GO was dried in a vacuum oven for 12-16 hours at 313.15K. A yield product of 0.6 g of PANI-GO was obtained.

2.3 Experimental Setup for Coating Application

The types of coating techniques are vital in determining the mechanical properties of the coating, such as thickness, uniformity, adhesion, and morphology. Therefore, this research study examines the coating method on substrates, which is dip coating. This method has its own unique and distinct benefits and limitations in its respective process in terms of quality control, scalability, and suitability for various substrates and coating materials. The method was selected to explore a range of coating application capabilities, allowing for a detailed comparison of their effectiveness in applying graphene-based nano-coatings on carbon steel substrates. Dip coating is one of the most frequent and suitable methods to coat a thin graphene film on a substrate, and for research purposes too (Figure 2). However, due to its inconsistent coating quality, it is not suitable for heavy and large industrial processes. The dip coating method process in this research study has 5 steps.

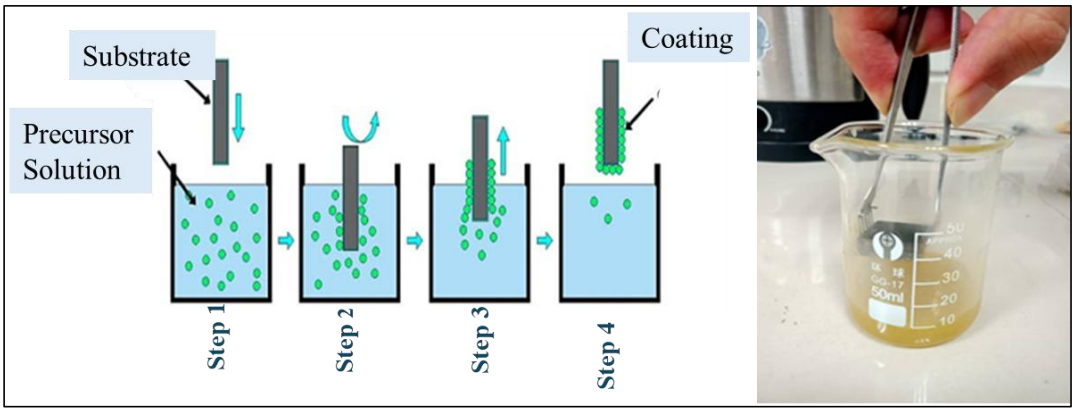

Figure 2. Dip coating basic process.

Firstly, 12 ml of epoxy resin was poured into each of 7 different beakers, for 7 different fillers. The first beaker was used for the 'control' coating parameter. The second beaker was filled with 0.2 wt% GO/Epoxy resin. The third beaker was filled with 0.2 wt% PPD-GO/Epoxy resin. The remaining beakers were filled with 0.1, 0.2, 0.4, and 0.6 wt% PANI-GO/Epoxy resin, respectively. Secondly, sonication in an ultrasonic bath for one hour was performed on all beakers to facilitate the stable and homogeneous dispersion of GO particles and remove bubbles throughout the epoxy resin matrix, thus preventing undesirable agglomeration. Thirdly, each beaker of epoxy resin matrix was dipped with a carbon steel substrate for 1 minute. Next, the substrates were lifted out from the epoxy coating solution and placed in an open surrounding at room temperature. By using a spatula, the coating solution on the surface of each substrate was properly adjusted for the surface to be completely coated. Lastly, the coated samples are cured in an oven for 2 hours at 60°C and dried at room temperature. The final coating thickness was about 750 ± 50µm for each sample. The drawback of this method is that the thin film coating may not have good quality, as it only requires simple preparation without any

complex equipment. Despite that, it can still produce products that can satisfy the applications for lower requirements at a much more reasonable price compared to other methods. Therefore, it can achieve better interfacial adhesion of epoxy coating towards the carbon steel substrates and a higher uniformity coating layer[30].

2.4 Characterization and Corrosion Testing Methods

Characterization of graphene-based nanocoating's on metal substrates can be carried out in several ways. X-ray Diffraction (XRD) is an excellent technique for analyzing the crystalline structure, phase composition, and lattice parameters of materials. It can provide information regarding the atomic and molecular structure of a material, specifically its crystallinity. When X-rays interact with the crystalline planes in a material, they diffract at specific angles according to Bragg's Law ($n\lambda=2d\sin\theta$). The X-ray diffraction studies of GO were performed under normal conditions and scanned in a 2θ range of 0° to 90°. The identification of graphene in the nanocoating would indicate that the coating's effectiveness depends on the properties of the graphene. A Fourier-Transform Infrared Spectrometer (FTIR) is used to identify functional groups present in a material by measuring the absorption of infrared radiation at different wavelengths. It provides a "fingerprint" spectrum of a compound, revealing the presence of specific chemical bonds and functional groups (e.g., O-H, C=O, C-H, C-O, C=C). The chemical bonding that was present during the synthesis was characterized using an FTIR employing the potassium bromide pellet method, ranging from 450 - 4000 cm-1. Scanning Electron Microscopy (SEM) is used to visualize the morphological surface structure of the coated substrate. Cracks, defects, and agglomeration of graphene can be detected through this method, along with evaluating the thickness of the coating and the uniformity of graphene particles dispersed. Information regarding the materials' particle size, shape, dispersion, porosity, and interface characteristics can be provided. The electrochemical behaviors and protective performance of GO, graphene-based composite nanocoating's, were tested using Electronic Impedance Spectroscopy (EIS) and salt immersion testing. The corrosion resistance of the composite nanocoating's was also compared and evaluated with other types of coatings through EIS. In general, EIS is used to evaluate electrochemical systems that detect the kinetics of the surface reactions using electrical response. It provides accurate kinetic and mechanical properties of a corroding system of a substrate. It is very suitable for use in applying nanocoating's on the substrate because it also evaluates the interaction of the metal-coating system with the corrosive environments and the degradation of highly resistant coatings. This means it can detect corrosion rates in the form of defects and porosity in the coating.

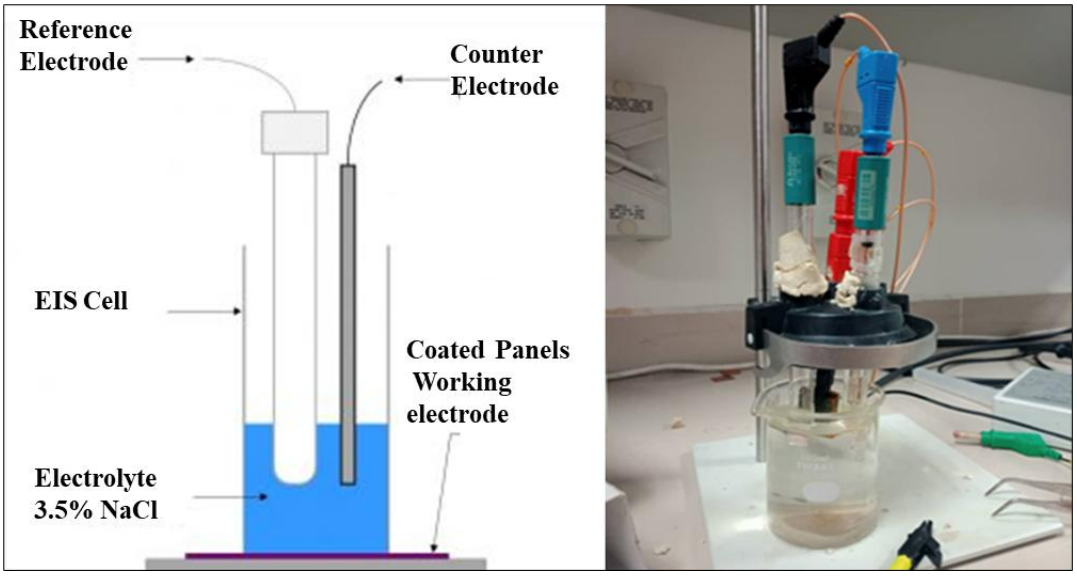

Figure 3. Corrosion testing via EIS.

The method involves connecting an AC voltage signal over a range of frequencies to the coated substrate immersed in an electrolyte. The resulting impedance is calculated by applying a sinusoidal potential to an electrochemical cell, and then the sinusoidal current is measured (Figure 3). EIS can quantify the barrier effect of graphene-based nanocoating by measuring the charge transfer resistance. A higher RCT value indicates that the coating is effectively preventing corrosion on the substrate. EIS detects defects like cracks, pinholes, grain boundaries, etc., by analyzing the impedance response at different frequencies. The presence of multiple time deviations in the Nyquist plots indicates the presence of defects. In terms of its long-lasting performance, the long-term corrosion protection performance of graphene nanocoating can be assessed when there are decreases or changes in other EIS parameters, which suggests degradation of the coating and reduced performance in its protective ability (Electrochemical Measurements: Electrochemical Impedance Spectroscopy [31, 32].

Salt immersion testing is a rapid corrosion test that produces a chemically corrosive reaction to coated samples as a way to evaluate the coating's protective finished product. The test duration depends on the performance of the coating to resist corrosion; the higher the corrosion resistance of the sample, the longer the time tested before any appearance of

corrosion takes place (Figure 4). The coated samples were placed in the salt immersion conditions, where they are continuously exposed to the salt solution (3.5% NaCl) at room temperature. The salt solution simulates a highly corrosive environment, similar to a harsh marine environment, which speeds up the corrosion process. Through visual inspection, the appearance of rust or any other corrosion products on the surface of the coated substrate indicates a failure of the coating to protect the material. This test is ideal for corrosion testing because it is very sensitive to coating defects. The test can also provide proven information about the adhesion and durability of the coating, as poor adhesion would lead to blistering or delamination of the coating and can be seen by the naked eye. Due to the visual results that are obtained after running the salt immersion test, the performance of graphene-based nanocoating's, other types of coatings, and uncoated samples can be compared and determined in terms of their effectiveness.

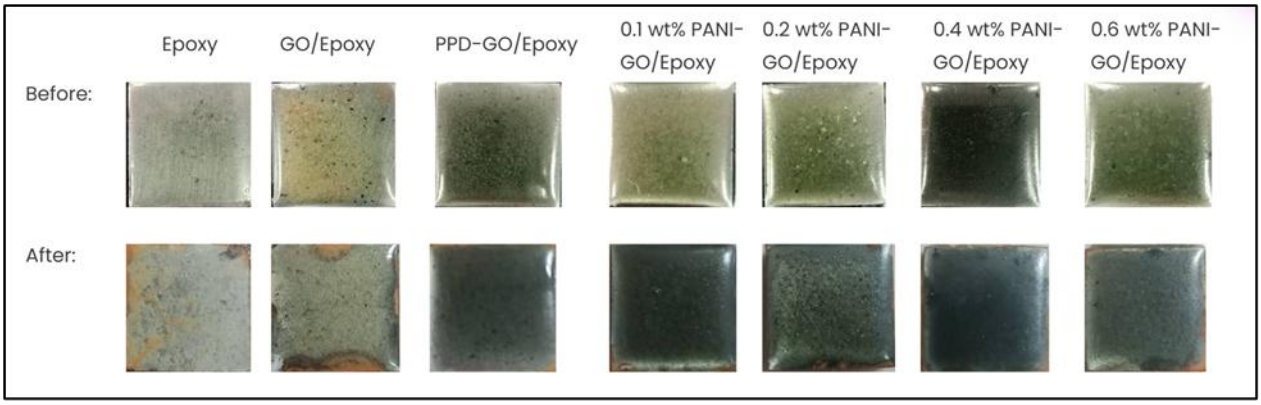

Figure 4. Illustration of result (before & after) of carbon steel substrates coated with different samples after being immersed in 3.5 wt% NaCl solution for 1 week.

3. Adsorption Energy and Temperature Influence

Graphene-based nanocoating's have gained significant attention for their corrosion resistance, particularly in offshore pipeline applications where materials face harsh conditions. These coatings serve as a protective layer over the underlying steel, enhancing its durability and lifespan. Materials Studio simulations have been utilized to gain insights into the adsorption energy of graphene nanocoating's, which is vital for understanding their corrosion resistance. The simulation results reveal variations in the adsorption energy of graphene on steel at different temperatures. This energy parameter quantifies the interaction between the graphene and steel surfaces; generally, higher adsorption energy indicates stronger adhesion, thereby improving the coating's protective capabilities. [33].

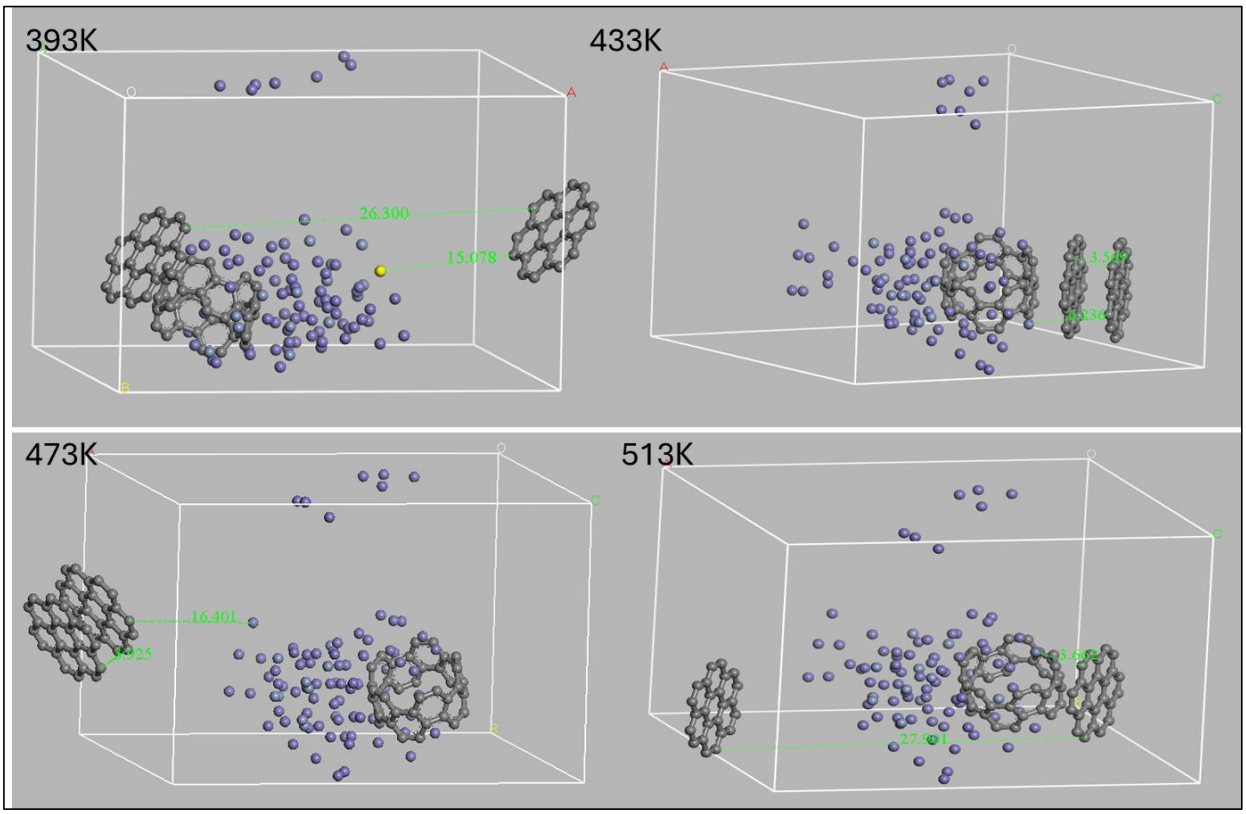

Figure 5. Adsorption Configuration of Graphene on steel at Different temperatures of 393, 433, 473, and 513K.

At 393 K, the adsorption energy is 446.03 Kcal/mol, suggesting a reasonable adhesion between graphene and the steel surface. As the temperature increases to 433 K (449.26 Kcal/mol), 473 K (454.73 Kcal/mol), and 513 K (446.99 Kcal/mol), the adsorption energy rises, indicating that the graphene layer is becoming more strongly attached to the steel substrate (Figure 6) [34]. This enhanced interaction is crucial for corrosion resistance, as a more robust adhesion reduces the likelihood of the graphene layer detaching or degrading, which would expose the steel to corrosive agents [35].

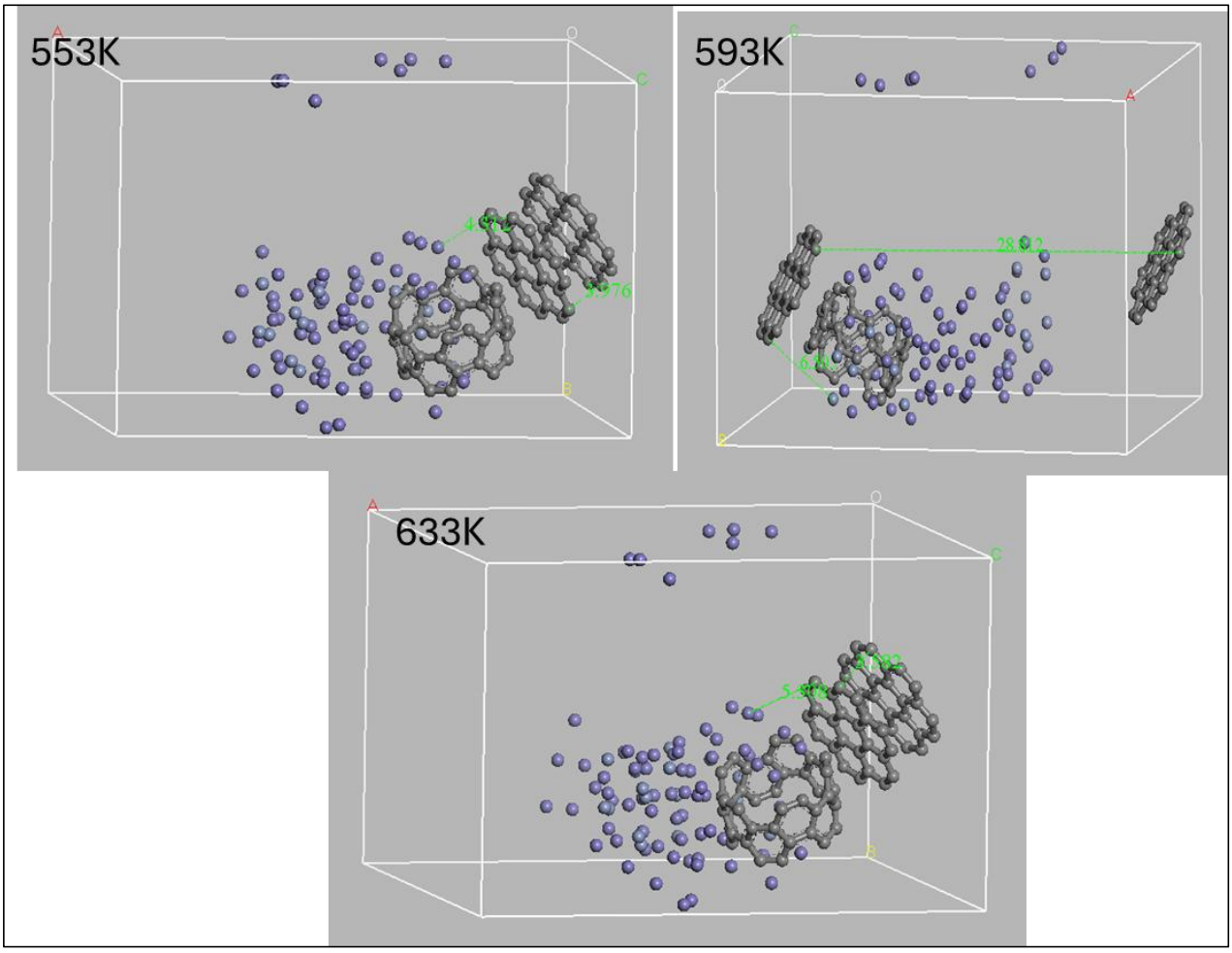

Figure 6. Adsorption Configuration of Graphene on steel at Different Temperatures of 553, 593, and 633K.

However, at higher temperatures of 533 K (453.33 Kcal/mol), 593 K (447.14 Kcal/mol), and 633 K (453.43 Kcal/mol), the adsorption energy fluctuates slightly. These variations suggest that, while the interaction between graphene and steel remains strong, some level of thermal instability or structural changes may occur at elevated temperatures [36]. Despite this fluctuation, the adsorption energies remain relatively high compared to lower temperatures, implying that the graphene coating continues to provide substantial protection against corrosion even in high-temperature environments. Van der Waals (vdW) energy is a critical factor in understanding the interactions between a graphene-based nanocoating and a steel surface, especially in the context of corrosion resistance for offshore pipeline applications (figure 7). The vdW energy quantifies the non-covalent interactions between the graphene sheet and the steel substrate, which are primarily driven by dispersion forces [37]. These interactions are essential because they influence the adhesion strength of the graphene coating, its stability, and its ability to protect steel from corrosion.

In the context of the Materials Studio simulation results at various temperatures, the Van der Waals energy shows noticeable fluctuations. At lower temperatures (393 K), the Van der Waals energy is -30.77 kcal/mol, indicating a relatively strong attractive interaction between the graphene coating and the steel surface [38]. As the temperature increases, the magnitude of the Van der Waals energy decreases, with values of -27.54 kcal/mol at 433 K, -22.07 kcal/mol at 473 K, and -29.81 kcal/mol at 513 K. At higher temperatures, the Van der Waals energy shows further variation, with values of -23.47 kcal/mol at 533 K, -29.66 kcal/mol at 593 K, and -23.37 kcal/mol at 633 K (Figure 8) [39]. These fluctuations suggest that the adhesion between the graphene coating and the steel surface becomes less stable as temperature rises, but the interaction is still relatively strong, providing effective corrosion protection.

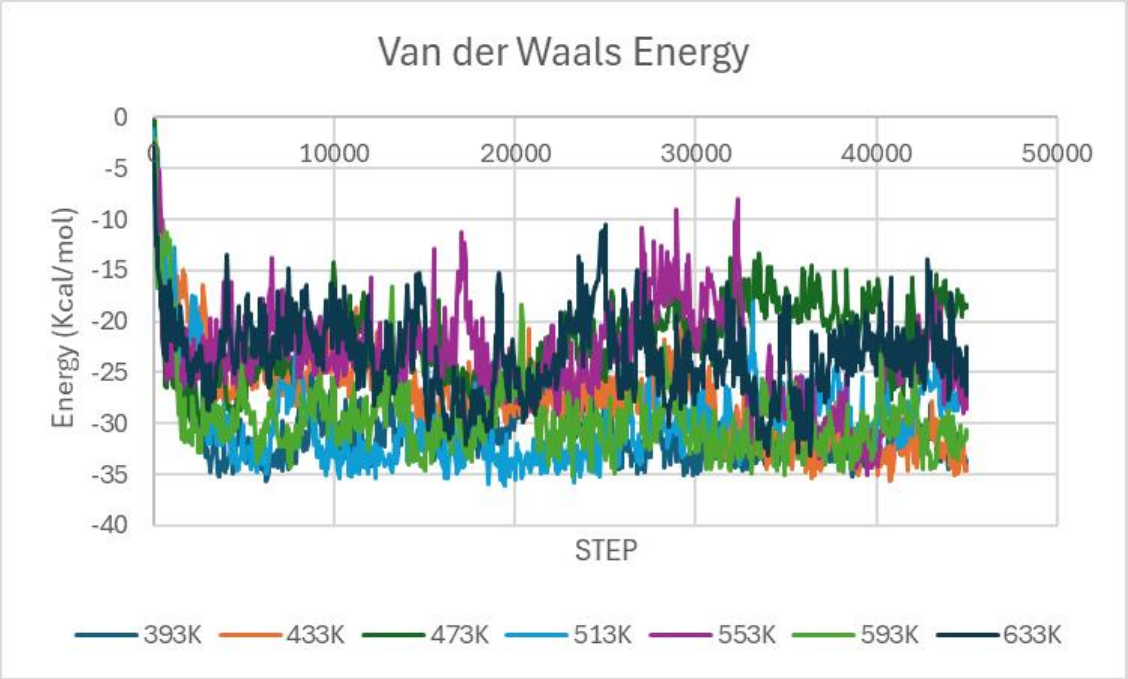

Figure 7. Van der Waals Energy of the graphene coated on steel for corrosion resistance at different temperatures.

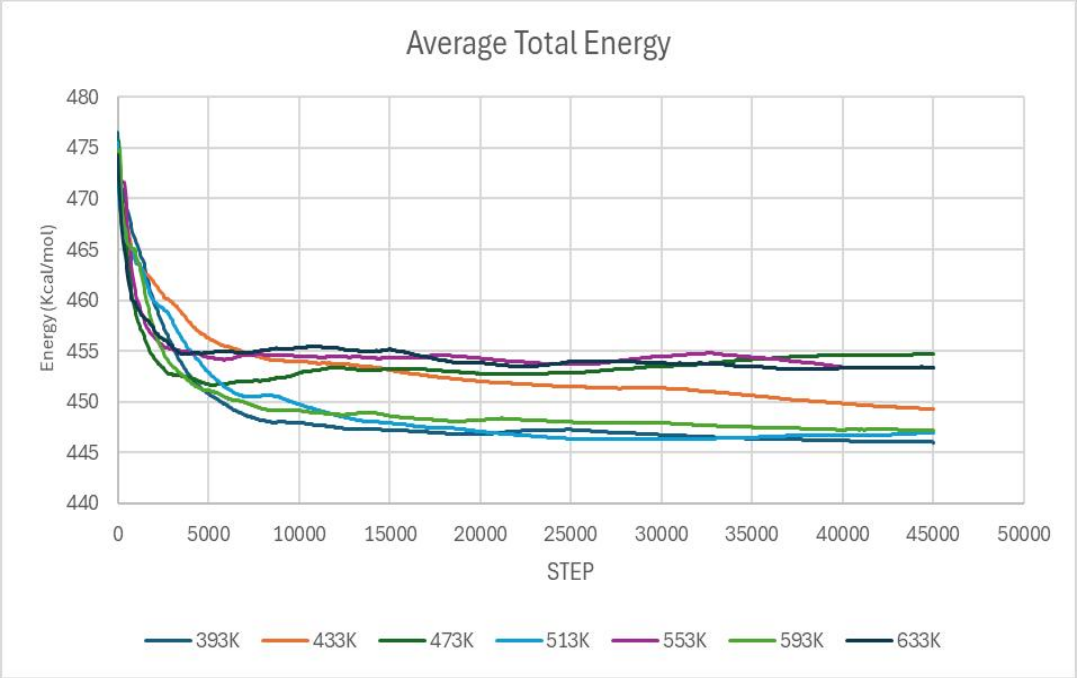

Figure 8. Average total energy of the graphene coated on steel for corrosion resistance.

The reduction in Van der Waals energy at higher temperatures may be due to the increased atomic vibrations within the system (Figure 7). At higher temperatures, the graphene sheet and the steel surface are more thermally excited, which can cause the non-covalent interactions to weaken slightly [40]. Despite these fluctuations, the negative values of Van der Waals energy at all temperatures indicate that graphene maintains a strong interaction with the steel surface, which is important for effective corrosion protection [41]. Graphene-based nanocoating's significantly enhance the corrosion resistance of steel, particularly in offshore pipeline applications where harsh environmental conditions prevail. The primary function of graphene in this context is to act as a protective barrier between the steel substrate and corrosive agents such as seawater, salts, and oxygen. Graphene is known for its remarkable chemical stability, impermeability to gases and liquids, and exceptional mechanical properties, all of which contribute to its ability to protect the steel from corrosion.

The Van der Waals energy directly influences the strength of the graphene-steel interaction, and by extension, the effectiveness of the graphene coating in preventing corrosion. The following points outline how this works:

- **Adhesion and Stability:** The Van der Waals energy represents the strength of the interaction between graphene and the steel surface. A strong, stable adhesion is essential for preventing the graphene layer from peeling off or degrading, which would expose the steel to corrosion. The values seen in the simulations suggest that the graphene coating forms a robust interaction with the steel substrate, even at higher temperatures.
- **Barrier Effect:** The graphene coating's impermeability, enhanced by the strong Van der Waals interaction, prevents moisture, oxygen, and other corrosive substances from reaching the steel surface. This greatly reduces the likelihood of electrochemical reactions that would otherwise lead to corrosion.
- **Thermal and Mechanical Resilience:** The strength of the Van der Waals interactions ensures that the graphene coating remains intact even at elevated temperatures. This is particularly important in offshore pipeline applications where temperature fluctuations are common. Despite some reduction in the interaction strength with increasing temperature, graphene still provides substantial protection due to its mechanical strength and the continued existence of significant Van der Waals interactions.
- **Enhanced Durability:** Even though the Van der Waals energy decreases at higher temperatures, graphene remains a highly durable and thermally stable material. It continues to protect the steel surface from corrosion by providing a continuous barrier that resists chemical and mechanical wear.

Graphene-based nanocoating's have garnered significant attention for their potential to enhance corrosion resistance in materials like steel, especially in harsh environments like offshore pipelines. The intramolecular energy data from the Materials Studio simulations across different temperatures provides insight into how the graphene layer interacts with the steel surface at various conditions, which is key to understanding its performance in corrosion prevention.

At the temperatures provided (393 K to 633 K), the intramolecular energy remains constant at 478.81 Kcal/mol. This suggests that the interaction between the graphene nanocoating and the steel surface is relatively stable across these temperature ranges. Such stability is crucial for corrosion resistance, as the graphene layer acts as a protective barrier against environmental factors such as water, salts, and gases that typically cause corrosion in steel (Figure 9) [18]. Graphene's role in enhancing corrosion resistance lies in its remarkable properties. It is known for its high electrical conductivity, mechanical strength, and impermeability. When applied as a coating on steel, graphene forms a robust and tightly bonded layer that can effectively block corrosive agents from reaching the underlying metal surface. The consistent intramolecular energy across the different temperatures suggests that graphene's protective capability is not significantly altered by temperature fluctuations in the studied range. This indicates that graphene-coated steel could maintain its integrity in varying offshore conditions, where temperatures can fluctuate.

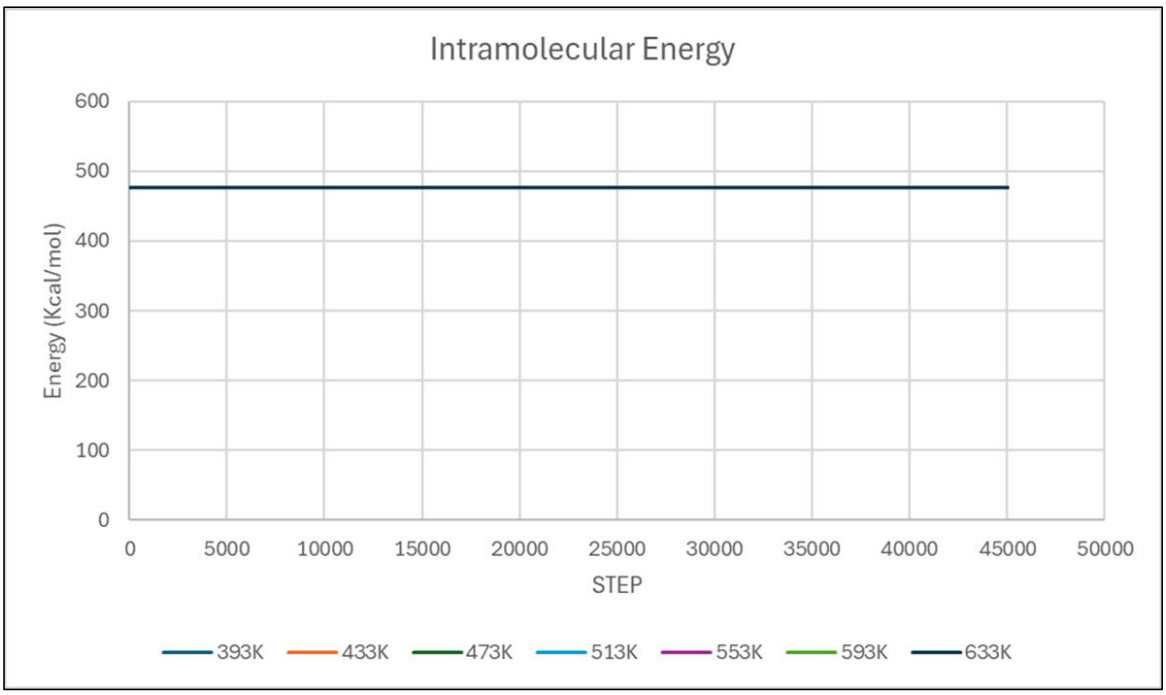

Figure 9. Intramolecular energy of the graphene coated on steel for corrosion resistance at different temperatures.

Furthermore, graphene's high chemical stability and resistance to oxidative degradation contribute to its durability under elevated temperatures. The fact that the graphene coating maintains a stable intramolecular energy even at higher temperatures (up to 633 K) suggests that it can provide long-term protection against corrosion without significant degradation or loss of effectiveness, making it an ideal material for offshore pipeline applications where steel is prone to rusting and other forms of corrosion.

3.1 XRD Analysis

A strong peak for GO is present at ~2θ ≈ 10.66° corresponding to the (001) reflection in Figure 10. This peak arises due to the increased interlayer spacing resulting from the introduction of oxygen-containing functional groups during the oxidation process, confirming successful oxidation of graphite to graphene oxide. The broad background hump around (10°–30° range) indicates disordered carbon structures, which are common in GO due to the presence of defects or other functional groups. The weaker peak at ~2θ ≈ 42–44° may correspond to residual graphitic contents, indicating incomplete oxidation or small crystalline domains. The Interlayer spacing d is ≈ 8.04 Å (0.804 nm) and is calculated using Bragg's Law; nλ = 2dsinθ, where λ is the X-ray wavelength of Cu Ka radiation (1.54 Å), d is the space between lattice planes, θ is the reflection angle, and n is equal to 1 [42]. The calculated value is typical for graphene oxide, as they have expanded interlayer spacing compared to graphite (~3.35 Å). The crystallite size of graphene oxide is about 4.0 nm and is calculated using the Scherrer Equation: D = Kλ / βcosθ, where K is the shape factor (typically 0.9), β is the FWHM in radians, θ is the Bragg angle in degrees, and D is the crystallite size.

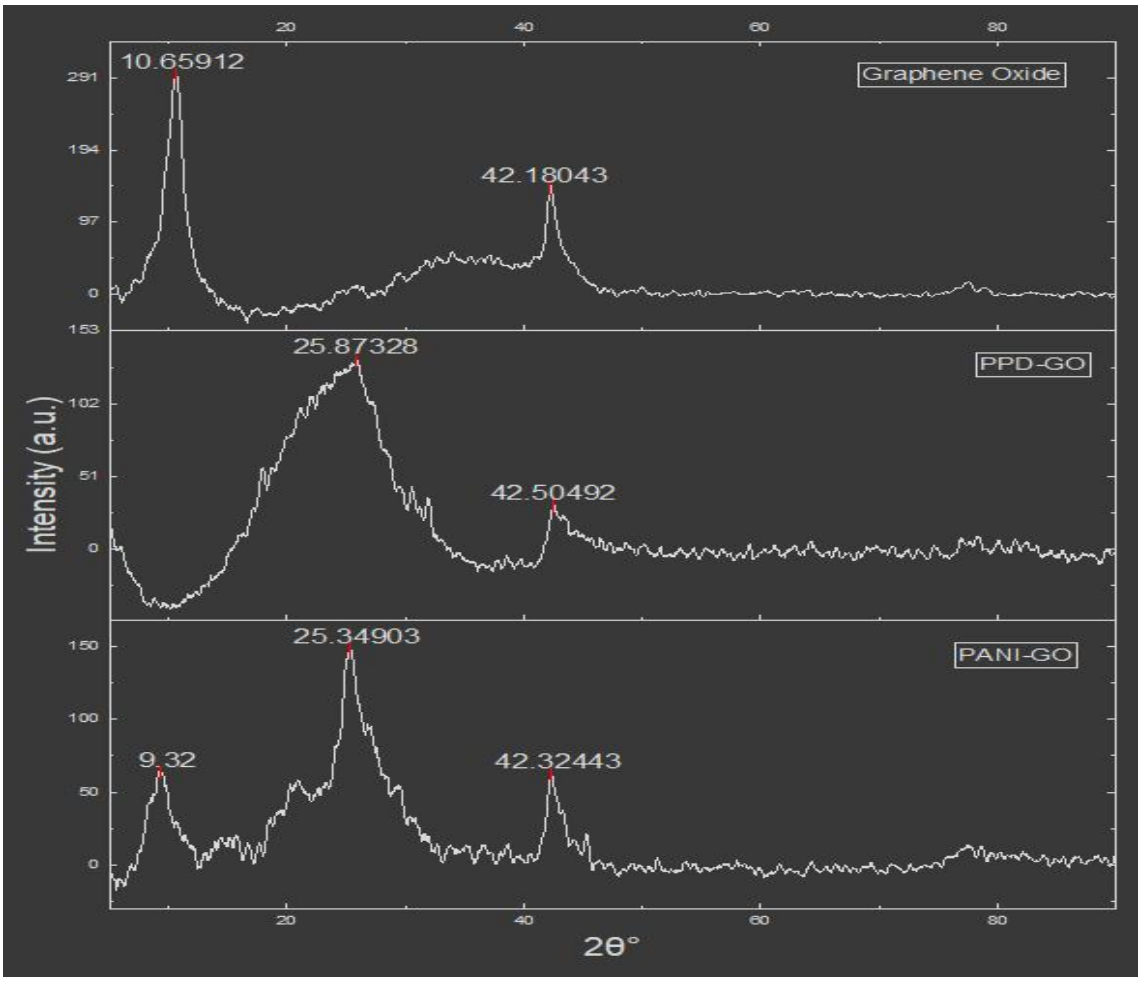

Figure 10. XRD patterns of GO, PPD-GO, and PANI-GO powder.

The sharp GO peak at about 10.66° vanishes in the case of PPD-GO (P-phenylenediamine-Graphene Oxide), and a broad peak appears at about 25.87° in Figure 10. The calculated d-spacing is d = 3.44A˚ (0.344 nm). This shows that PPD was successful in reducing GO and/or intercalating/exfoliating. The removal of oxygen functions and subsequent restacking of the graphene layers, leading to a more graphite-like structure, or the creation of a new composite where PPD is introduced, are suggested by the shift to a higher 2θ value, which indicates a smaller d-spacing. This peak's broadness suggests the presence of tiny domain sizes or a less organized structure than that of pristine GO. Additionally, there is still a peak at around 42.50° that is comparable in location to the GO pattern, indicating that the in-plane ordering of the graphene framework has been retained. The presence of some residual graphene oxide (GO) or a particular interaction and arrangement of PANI with GO, resulting in a slightly increased interlayer spacing compared to the decreased GO, is suggested by the modest, relatively broad peak for PANI-GO (Polyaniline-Graphene Oxide) observed at approximately 9.32° in Figure 10. A noticeable broad peak has moved to about 25.35°, which is very suggestive of an effective PANI-GO interaction. The calculated d-spacing is d = 3.52A˚ (0.352 nm). In this interaction, GO is reduced and/or a PANI-GO composite is formed, in which the PANI chains restack or partially exfoliate the GO layers. The amorphous nature of PANI and the re-stacked graphene layers are characterized by this broad peak. The fact that the peak at about 42.32° is still there indicates that the PANI-GO composite has mostly preserved the underlying graphene lattice structure.

Graphene Oxide (GO) has an extended structure (d-spacing ~8.28 Å), according to the XRD patterns. The GO structure is drastically altered when coupled with PPD or PANI. Its distinctive peak vanishes and is replaced by larger peaks at 25–26° (2θ), with d-spacings of roughly 3.44–3.52 Å. This suggests that a more compact, reduced-GO-like structure has resulted from the PPD and PANI's successful interaction with and reduction of the GO. A constant peak at about 42° (2θ) indicates that the underlying graphene sheet structure is generally intact, even as the materials grow more disordered (wide peaks).

3.2 FTIR Analysis

For GO, the spectrum in Figure 11 (GO) shows broad and intense bands, which are typical for graphene oxide due to the presence of various oxygen-containing functional groups and adsorbed water. The broad and intense peak occurring at 3394.90 cm-1 corresponds to the O-H stretching vibrations of hydroxyl groups (-OH) and carboxylic acid groups (-COOH). The prominent peak at 1700 cm-1 is a high indicator of the C=O stretching vibration from carboxylic acid groups (-COOH), showing successful oxidation, as carboxylic acid groups are formed at the edges of graphene sheets during oxidation. The peak at 1626.28 cm-1 can be formed due to several possibilities. C=C stretching vibrations from unoxidized aromatic domains, indicating graphitic domains remain in the structure, and O-H bending vibrations of adsorbed water molecules (H-O-H scissoring). The peak at 1415.65 cm-1 can be assigned to O-H bending vibrations from carboxylic acids and hydroxyl groups, supporting the presence of hydroxyl and carboxylic acid functionalities. The strong peak at 1260.53 cm-1 is typically assigned to the C-O stretching vibration from epoxy groups (C-O-C). This is crucial to indicate the presence of oxygen functionalities within the graphene basal plane due to oxidation. The broad peak at 1092.23 cm-1 is also associated with C-O stretching vibrations, primarily from epoxy and alkoxyl (C-OH) groups.

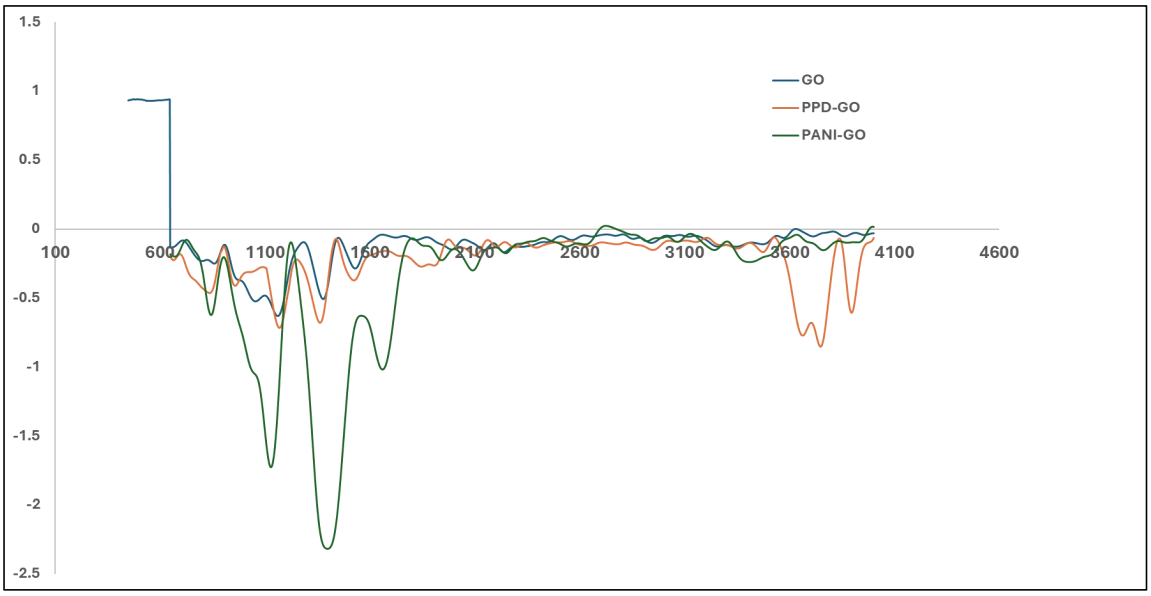

Figure 11. FTIR spectra of GO, PPD-GO, and PANI-GO.

For p-Phenylenediamine Graphene Oxide (PPD-GO), the peaks observed from the spectrum in Figure 11 (PPD-GO) indicate the presence of various functional groups resulting from the functionalization of GO with PPD. The peaks occurring at 2929.36 / 2861.09 cm-1 are associated with -CH2 asymmetric/symmetric stretching, indicating of alkyl chains from organic modification, eg, PPD structure. The peaks at 1625.70 / 1604.73 are assigned to C=C (aromatic) or C=O (carbonyl) stretching, which shows the presence of aromatic rings from PPD or conjugated carbon framework in GO. The peaks observed at 1573.04 / 1543.93 cm-1 show N-H bending or C-N stretching, which confirms the incorporation of PPD (having -NH_2 groups), a strong indication of amine functional groups. The peak at 1184.37 cm-1 is associated with C-O-C stretching (epoxy/ether), which confirms the presence of residual oxygen functionality from GO. The peaks at 819.56 / 739.01 cm-1 assign the aromatic C-H out-of-plane bending, confirming PPD aromatic substitution.

The successful creation of a polyaniline-graphene oxide (PANI-GO) composite is shown by the FTIR spectrum in Figure 11 (PANI-GO). The presence of both GO's hydroxyl groups and PANI's amine groups is shown by the extremely broad and intense peak at 3410.13 cm^{-1}, which suggests that the two materials have significant hydrogen bonding interactions. The organic origin of PANI is established by the peak at 2923.64 cm^{-1}, which validates the C-H stretching vibrations from its aromatic rings. The quinoid ring units in PANI, which are essential for its conductive qualities, are indicated by the strong peak at 1560.48 cm^{-1}, while the benzenoid ring units are confirmed by the peak at 1476.68 cm^{-1}. Taken together, these two values indicate that PANI is in its emeraldine form. The C-N stretching vibrations inside the PANI structure are indicated by the 1289.63 cm^{-1} peak, which further confirms their existence. Both protonated C-N bonds in PANI, which are crucial for conductivity, and C-O-C (epoxy) groups from GO, which show that GO has retained some oxygen functions, are suggested by the 1232.49 cm^{-1} peak. Crucially, the "polaron band," a prominent

peak at 1103.33 cm^{-1}, offers unmistakable proof that the polyaniline in the composite is in its electrically conducting emeraldine salt form. Lastly, the out-of-plane C-H bending in PANI's aromatic rings is shown by the 799.52 cm^{-1} peak, indicating the structural integrity of the compound within the composite. All things considered, the co-occurrence and properties of these peaks validate that a well-integrated polyaniline-graphene oxide composite with conducting polyaniline was successfully formed.

3.3 SEM Analysis

In Figure 12 (a), the image is a Scanning Electron Microscopy (SEM) micrograph of Graphene Oxide (GO). The magnification is indicated as x5.0k (5000 times), and the scale bar represents 20 µm. The image shows a material with a visible lamellar (layered) and highly wrinkled or crumpled morphology. This is characteristic of GO, as the oxidation process introduces functional groups that disrupt the sp2 hybridization of graphite, leading to exfoliation and the formation of these wrinkled sheets. Significant evidence of agglomeration or aggregation is shown in the GO sheets. Instead of perfectly flat, individual sheets, we see clumps and stacks of the material. This is common for GO, especially if it hasn't been highly dispersed or if it has undergone drying without proper measures to prevent restacking. The individual sheets appear to be somewhat interlocked or piled upon each other. The individual "flakes" or agglomerates of GO display irregular shapes and a range of sizes, consistent with the exfoliation process, where various sizes of GO sheets can be produced. While not explicitly clear due to the agglomeration, the wrinkled and stacked nature suggests the presence of interstitial spaces and potentially a high surface area, which is a desirable property for many GO applications. Despite the wrinkled nature, the overall appearance suggests a relatively dense packing of the GO material within the observed area, rather than a highly porous, open framework. This could be due to the drying process, sample preparation, or inherent properties of this GO synthesis.

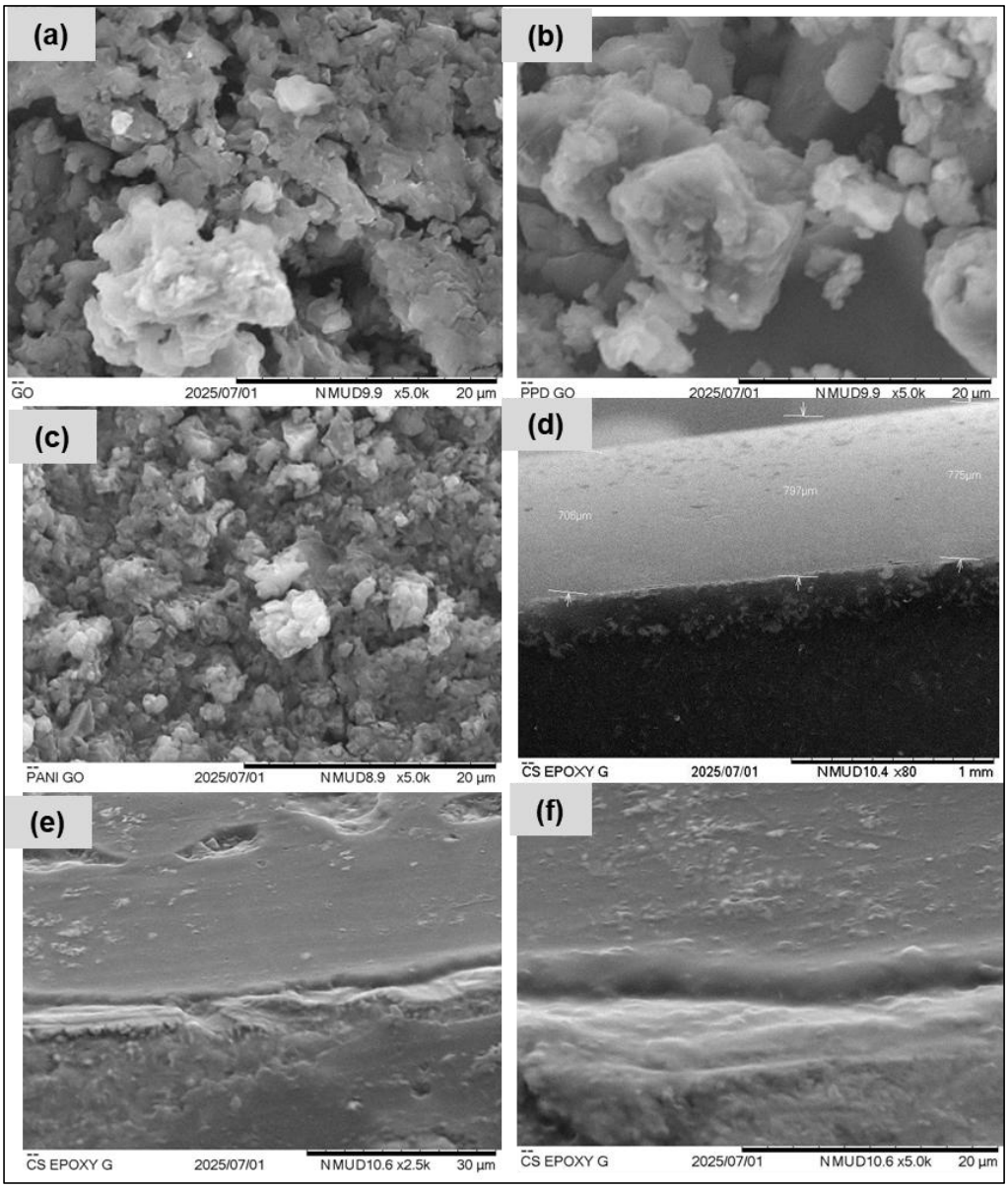

Figure 12. SEM images of (a) GO (b) PPD-GO (c) PANI-GO (d, e, f) cross sections of GO/epoxy coating on carbon steel substrate at different magnifications.

In Figure 12 (b), PPD-GO is Graphene Oxide (GO) that has been functionalized or reacted with p-phenylenediamine. The magnification is x5.0k (5000 times), and the scale bar indicates 20 μm. Compared to the typical morphology of pristine GO (which often appears as crumpled, sheet-like structures), this image of PPD GO shows more distinct, chunkier, and somewhat aggregated "particle-like" formations. The individual structure appears less like thin, exfoliated sheets and more like compacted, irregular blocks or agglomerates. There's a noticeable degree of aggregation and compaction of the material. The original layered structure of GO, if present, is less discernible. This could be due to several factors related to the p-phenylenediamine modification, like cross-linking, where PPD, being a diamine, can act as a cross-linking agent between GO sheets, leading to a more rigid and aggregated structure. This is a common strategy to modify GO's properties and morphology. The reaction with p-phenylenediamine might also induce some degree of reduction of GO to reduced graphene oxide (rGO), which can lead to restacking of the graphene layers, contributing to the denser, more aggregated appearance. The introduction of PPD functional groups could facilitate stronger interactions (e.g., hydrogen bonding, pi-pi stacking) between GO sheets, promoting their aggregation. The observed "particles" are highly irregular in shape and vary in size, ranging from smaller agglomerates to larger, more substantial chunks. While still rough, the extensive, delicate wrinkling often seen in pristine GO sheets appears to be less dominant. The structures seem more solid and less prone to the fine, sheet-like folds, which further supports the idea of cross-linking or reduction leading to a more consolidated structure. The surface of these aggregated particles appears rough, indicating the presence of numerous smaller features or the composite nature of the agglomerates.

In Figure 12 (c), the image is a "PANI GO," a composite or functionalized material involving Polyaniline (PANI) and Graphene Oxide (GO). The magnification is x5.0k (5000 times), and the scale bar represents 20 μm. The most striking feature is the highly aggregated and dense particulate morphology. The material appears as an assembly of irregular, somewhat chunky particles and agglomerates, rather than distinct individual sheets. Unlike pristine GO, where individual wrinkled sheets might be discernible, the characteristic lamellar (layered) or highly wrinkled features of GO sheets are largely obscured in this image. This suggests that the GO sheets are either intimately wrapped by PANI, acting as templates for PANI growth, or are highly aggregated with PANI. While definitive identification of PANI's typical fibrous or granular morphology is challenging at this magnification amidst the GO, the overall compact and somewhat rough texture could be attributed to the presence of PANI. Polyaniline often forms granular or rod-like structures, and when combined with GO, it can coat or intertwine with the GO sheets. The irregular, dense particles could be PANI growing on or encapsulating the GO. There might be some heterogeneity in the size and compactness of the agglomerates. Some regions appear denser and more fused, while others show slightly more open spaces, though still highly aggregated. The surfaces of the agglomerates appear rough and irregular, consistent with a composite material where two different components (PANI and GO) are combined, leading to a complex surface topography. The PANI GO composite is significantly more aggregated and particulate, with the individual GO sheet morphology almost entirely lost. While both PANI GO and PPD GO exhibit aggregated particulate structures, PANI GO appears even more densely packed and homogeneous in its "lumpiness" than PPD GO, which still showed some hints of distinct, though aggregated, blocks. This could suggest a more extensive coating or incorporation of PANI around the GO.

The shape and structural integrity of the GO-epoxy coating on the carbon steel substrate are thoroughly revealed by the SEM images in Figure 12 (d), (e), (f). Measured between 700 and 800 micrometers, observations made at different magnifications show a consistently thick covering, indicating a strong protective layer. Importantly, there are no obvious indications of delamination, cracking, or large voids at the interface between the epoxy coating and the carbon steel substrate, indicating good interfacial bonding that is essential for long-term durability. Higher magnification photos show a faint, textured layer close to the substrate contact, which may indicate a localized enrichment or preferential distribution of graphene oxide in this crucial area, even if the bulk epoxy matrix appears to be mostly homogeneous and free of significant flaws. These magnifications, however, do not discern the precise dispersion and morphology of individual GO flakes throughout the entire epoxy matrix, indicating either highly exfoliated forms or the need for higher-resolution analytical techniques. Overall, the coating shows strong interfacial bonding and good structural integrity, both of which are critical for its expected performance in corrosion protection applications.

4. Conclusion

Graphene-based nanocoating’s show significant potential as corrosion-resistant layers for offshore pipelines exposed to harsh environments. Simulations revealed strong adhesion between graphene and steel with high adsorption energies across various temperatures, ensuring the integrity of the graphene layer against thermal fluctuations. Minor reductions in Van der Waals (VdW) energies were observed at higher temperatures, but these remained negative, signifying stable attractive forces necessary for coating durability. The intramolecular energy of graphene remained consistent, demonstrating its thermal resilience and structural stability. Structural and chemical characterization of graphene oxide (GO) through XRD confirmed successful oxidation, as indicated by a distinct diffraction peak at $2\theta \approx 10.66°$ and an interlayer spacing increase to 8.04 Å compared to graphite's ~3.44 Å. FTIR analysis identified oxygenated functional groups, including O–H and C=O bonds, with SEM showing wrinkled and agglomerated GO sheets that ensure extensive surface coverage.

The introduction of p-phenylenediamine (PPD) significantly altered the structure of GO. XRD peak shifts to $2\theta \approx 25.87°$ indicated layer reduction, while FTIR showed new signals affirming PPD integration, coupled with SEM images of denser morphologies consistent with structural changes. Polyaniline-functionalized GO (PANI-GO) displayed

characteristic FTIR peaks confirming its emeraldine salt form, alongside broad XRD peaks suggesting exfoliation and partial GO reduction. SEM micrographs depicted aggregated, encapsulated structures reflecting a uniform PANI coating. Collectively, the composites GO, PPD-GO, and PANI-GO demonstrate exceptional adhesion, chemical stability, and a variety of functional groups, ensuring prolonged corrosion resistance and validating their capabilities as efficient coatings for offshore pipelines, ultimately enhancing service longevity and reducing maintenance expenses.

Generative AI statement

The authors declare that no Gen AI was used in the creation of this manuscript.

References

[1] Canbaz CH, Aydin H, Canbaz E, Akberov I, Aksahan F, Hussain A, et al. A comprehensive review and status of renewable resources and oil & gas under the supply and demand dynamics in the world. in SPE Europec featured at EAGE Conference and Exhibition? 2021. SPE. DOI: 10.2118/205116-MS
[2] Newell R, Raimi D, Aldana G. Global energy outlook 2019: The next generation of energy. Resources for the Future, 2019, 1(8), 1-37.
[3] Shams S, Prasad DR, Imteaz MA, Khan MMH, Ahsan A, Karim MR. An assessment of environmental impact on offshore decommissioning of oil and gas pipelines. Environments, 2023, 10(6), 104. DOI: 10.3390/environments10060104
[4] Xia R, Jia C, Garbatov Y. Deterioration of marine offshore structures and subsea installations subjected to severely corrosive environment: A review. Materials and Corrosion, 2025, 76(6), 758-775. DOI: 10.1002/maco.202314050
[5] Obike A, Uwakwe K, Abraham E, Ikeuba A, Emori W. Review of the losses and devastation caused by corrosion in the nigeria oil industry for over 30 years. International Journal of corrosion and scale inhibition, 2020, 9(1), 74-91. DOI: 10.17675/2305-6894-2020-9-1-5
[6] Lu H, Xi D, Qin G. Environmental risk of oil pipeline accidents. Science of the total environment, 2023, 874, 162386. DOI: 10.1016/j.scitotenv.2023.162386
[7] Singh AP, Saxena R, Saxena S, Maurya NK. The future of protection: Unleashing the power of nanotech against corrosion. Asian Journal of Current Research, 2024, 9(3), 23-44. DOI: 10.56557/ajocr/2024/v9i38727
[8] Zamindar S, Mandal S, Murmu M, Banerjee P. Unveiling the future of steel corrosion inhibition: A revolutionary sustainable odyssey with a special emphasis on n+-containing ionic liquids through cutting-edge innovations. Materials Advances, 2024, 5(11), 4563-4600. DOI: 10.1039/D4MA00156G
[9] Sparks S, Nanotechnology: Business applications and commercialization. CRC press, 2017. DOI: 10.1201/b11849
[10] Sahudin MR, Zourob M, Noor Akashah MH, Abdul Rani R, Makhsin SR. Physical properties of graphene. Journal of Mechanical Engineering, 2023, 12(1), 225-267. DOI: 10.24191/jmeche.v12i1.24649
[11] Gao Y, Yin F, Li S, Zhao X, Yao H, Zhang L. Hydrate deposition and blockage mechanism in undulating pipes of deepwater gas transmission pipelines. Energy & Fuels, 2024, 38(21), 20618-20628. DOI: 10.1021/acs.energyfuels.4c04239
[12] Assad H, Lone IA, Sihmar A, Kumar A, Kumar A. An overview of contemporary developments and the application of graphene-based materials in anticorrosive coatings. Environmental science and pollution research, 2023, 1-20. DOI: 10.1007/s11356-023-30658-7
[13] Assad H, Lone IA, Sihmar A, Kumar A, Kumar A. An overview of contemporary developments and the application of graphene-based materials in anticorrosive coatings. Environ Sci Pollut Res 32, 16958–16977 (2025). https://doi.org/10.1007/s11356-023-30658-7
[14] Zhou Y, Li Q, Atrens A, Wu L. Graphene-based anti-corrosion coatings on magnesium alloys: A review. Surface Engineering, 2023, 39(4), 392-412. DOI: 10.1080/02670844.2023.2227441
[15] Hussain AK, Sudin I, Basheer UM, Yusop MZM. A review on graphene-based polymer composite coatings for the corrosion protection of metals. Corrosion Reviews, 2019, 37(4), 343-363. DOI: 10.1515/corrrev-2018-0097
[16] Ollik K, Lieder M. Review of the application of graphene-based coatings as anticorrosion layers. Coatings, 2020, 10(9), 883. DOI: 10.3390/coatings10090883
[17] Ehsani A, Heidari AA, Sajedi M. Graphene and graphene/polymer composites as the most efficient protective coatings for steel, aluminum and copper in corrosive media: A review of recent studies. The Chemical Record, 2020, 20(6), 467-493. DOI: 10.1002/tcr.201900021
[18] Wen G, Bai P, Tian Y. A review of graphene-based materials for marine corrosion protection. Journal of bio-and tribo-corrosion, 2021, 7(1), 27. DOI: 10.1007/s40735-020-00456-6
[19] Sharma A, Sharma S. Graphene-based polymer coatings for preventing marine corrosion: A review. Journal of Coatings Technology and Research, 2023, 20(2), 413-432. DOI: 10.1007/s11998-022-00730-x
[20] Sabet M. Unveiling transformative potential: Recent advances in graphene-based polymer composites. Iranian Polymer Journal, 2024, 33(11), 1651-1665. DOI: 10.1007/s13726-024-01337-2
[21] Sabet M, Sabet S. Biocompatible graphene polymer composites: New frontiers in biomedical and environmental applications. Polymer-Plastics Technology and Materials, 2025, 64(9), 1282-1314. DOI: 10.1080/25740881.2025.2460206
[22] Zhang XF, Wang N, Li XD, Li X, Wang CX. Molecular dynamics study of the corrosion protection improvement of superhydrophobic dodecyltrimethoxysilane film on mild steel. Journal of Molecular Graphics and Modelling, 2024, 126, 108626. DOI: 10.1016/j.jmgm.2023.108626
[23] Kumar P. Recent progress in computational techniques in various coating materials. Coating materials: Computational aspects, applications and challenges, 2023, 217-228. DOI: 10.1007/978-981-99-3549-9_10
[24] Chan EJ, Neumann MA. Evaluation of general and tailor made force fields via x-ray thermal diffuse scattering using molecular dynamics and monte carlo simulations of crystalline aspirin. Journal of Chemical Theory and Computation, 2018, 14(4), 2165-2179. DOI: 10.1021/acs.jctc.7b01073
[25] Jannat M. Understanding ion rejection mechanism of freeze desalination by molecular dynamics simulation. 2024. DOI: 10.26076/5efc-f077

[26] Mhamdi Alaoui H, Zhao C, Niu W, Yang Z. Investigating temperature effects on the shear behavior of clays: Molecular dynamics simulations. Canadian Geotechnical Journal, 2024, 62, 1-23. DOI: 10.1139/cgj-2024-0471
[27] Zhou Y, Yan T, Pan W. Study on the sorption mechanism of middle-low temperature sorption thermal storage materials from the microscale simulation: A review. International Journal of Energy Research, 2021, 45(7), 9719-9752. DOI: 10.1002/er.6495
[28] Chandra DK, Kumar A, Mahapatra C. High-precision multistage molecular dynamics simulations and quantum mechanics investigation of adsorption mechanisms of cerium-based H_3BTC MOF (Ce-H_3BTC-MOF) on pristine and functionalized carbon nanotubes. Langmuir, 2025. DOI: 10.1021/acs.langmuir.5c01011
[29] Al-Ruqeishi MS, Mohiuddin T, Al-Moqbali M, Al-Shukaili H, Al-Mamari S, Al-Rashdi H, et al. Graphene oxide synthesis: Optimizing the hummers and marcano methods. Nanoscience and Nanotechnology Letters, 2020, 12(1), 88-95. DOI: 10.1166/nnl.2020.3074
[30] Tian H, Wei S, Chen Y, Tong H, Liu Y, Xu B. Surface remelting treated high velocity arc sprayed fenicralbre coating by tungsten inert gas. Physics Procedia, 2013, 50, 322-327. DOI: 10.1016/j.phpro.2013.11.051
[31] Microscopy SE, Nanoscience instruments. 2024
[32] Lazanas A, Prodromidis M. Electroanalysis of bromate via an autocatalytic redox mediation cycle in finite length diffusion regime in porous electro activated riboflavin impregnatedketjen black modified screen-printed electrode. Available at SSRN 4799034. DOI: 10.2139/ssrn.4799034
[33] Parhizkar N, Shahrabi T, Ramezanzadeh B. A new approach for enhancement of the corrosion protection properties and interfacial adhesion bonds between the epoxy coating and steel substrate through surface treatment by covalently modified amino functionalized graphene oxide film. Corrosion science, 2017, 123, 55-75. DOI: 10.1016/j.corsci.2017.04.011
[34] Das S, Lahiri D, Lee DY, Agarwal A, Choi W. Measurements of the adhesion energy of graphene to metallic substrates. Carbon, 2013, 59, 121-129. DOI: 10.1016/j.carbon.2013.02.063
[35] Healy B, Yu T, da Silva Alves D, Breslin CB. Review of recent developments in the formulation of graphene-based coatings for the corrosion protection of metals and alloys. Corrosion and Materials Degradation, 2020, 1(3), 15. DOI: 10.3390/cmd1030015
[36] Liu F, Wang M, Chen Y, Gao J. Thermal stability of graphene in inert atmosphere at high temperature. Journal of Solid State Chemistry, 2019, 276, 100-103. DOI: 10.1016/j.jssc.2019.04.008
[37] Zhan J, Lei Z, Zhang Y. Non-covalent interactions of graphene surface: Mechanisms and applications. Chem, 2022, 8(4), 947-979. DOI: 10.1016/j.chempr.2021.12.015
[38] Sekkal W, Izadifar M, Zaoui A, Ukrainczyk N, Koenders E. Theoretical investigation of protective graphene-coated metakaolin geopolymer interface under moisture and chemical composition effects. Powder Technology, 2023, 430, 119007. DOI: 10.1016/j.powtec.2023.119007
[39] Neumann MA, Perrin MA. Energy ranking of molecular crystals using density functional theory calculations and an empirical van der waals correction. The Journal of Physical Chemistry B, 2005, 109(32), 15531-15541. DOI: 10.1021/jp050121r
[40] Wang Y, Yang C, Mai YW, Zhang Y. Effect of non-covalent functionalisation on thermal and mechanical properties of graphene-polymer nanocomposites. Carbon, 2016, 102, 311-318. DOI: 10.1016/j.carbon.2016.02.069
[41] Moradi M, Rezaei M. Corrosion protection mechanisms of graphene oxide-reinforced polypropylene coating for mild carbon steel by advanced molecular dynamics simulations with emphasis on resistance to water and chloride ion penetration. Journal of Molecular Liquids, 2022, 367, 120389. DOI: 10.1016/j.molliq.2022.120389
[42] Akl AAS. Estimation of the lattice parameters, crystallite size and internal micro strain of $Cu_{1-x}In_xSe_2$ Thin Films by Williamson-Hall Method. Determinations in nanomedicine & nanotechnology, 2020, 1(5). DOI: 10.31031/DNN.2020.01.000523